

Anomalous Charge Transport in Conjugated Polymers Reveals Underlying Mechanisms of Trapping and Percolation

Sonya A. Mollinger,[†] Alberto Salleo,[†] and Andrew J. Spakowitz^{*,†,‡,§,||}

[†]Department of Materials Science and Engineering, Stanford University, Stanford, California 94305, United States

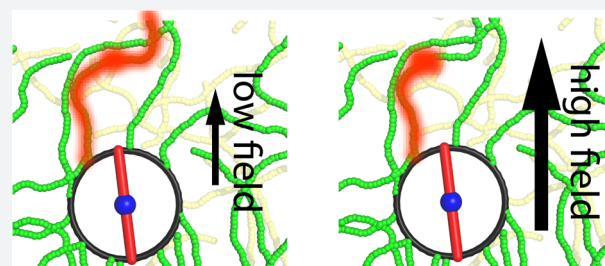
[‡]Department of Chemical Engineering, Stanford University, Stanford, California 94305, United States

[§]Department of Applied Physics, Stanford University, Stanford, California 94305, United States

^{||}Biophysics Program, Stanford University, Stanford, California 94305, United States

Supporting Information

ABSTRACT: While transport in conjugated polymers has many similarities to that in crystalline inorganic materials, several key differences reveal the unique relationship between the morphology of polymer films and the charge mobility. We develop a model that directly incorporates the molecular properties of the polymer film and correctly predicts these unique transport features. At low degree of polymerization, the increase of the mobility with the polymer chain length reveals trapping at chain ends, and saturation of the mobility at high degree of polymerization results from conformational traps within the chains. Similarly, the inverse field dependence of the mobility reveals that transport on single polymer chains is characterized by the ability of the charge to navigate around kinks and loops in the chain. These insights emphasize the connection between the polymer conformations and the transport and thereby offer a route to designing improved device morphologies through molecular design and materials processing.



transport and thereby offer a route to designing improved device morphologies through molecular design and materials processing.

Conjugated polymers are a widely researched material in the field of flexible and low-cost electronic devices. These polymers are currently used in organic solar cells^{1,2} and as the active material in thin-film organic transistors.^{3,4} Transistors based on semiconducting polymers have reached mobility values exceeding that of amorphous silicon and comparable to that of single crystals of organic small molecules.^{5,6} Unlike inorganic or ordered organic materials, typical polymer devices are made of semicrystalline films, which contain both significant regions of amorphous material as well as paracrystalline regions of ordered aggregated polymers.

Several features of transport in conjugated polymers recall properties of inorganic amorphous semiconductors. For example, the widely observed Poole–Frenkel effect^{7,8} dictates that the mobility μ increases exponentially with the square root of the field strength F , i.e., $\mu \sim \exp(\beta\sqrt{F})$, where β is a positive constant. Transport is also temperature-activated where the mobility follows an exponential trend in the inverse of temperature. These similarities have encouraged researchers to leverage experimental insights and theoretical models for inorganic amorphous semiconductors in establishing the fundamental design principles for charge transport in conjugated polymer materials.

Their macromolecular nature however makes conjugated polymers fundamentally different from amorphous inorganic semiconductors. The ubiquitous presence of polymers in a broad spectrum of materials applications is driven by desirable properties that directly arise from macromolecular structural

features. Polymer entanglement at large molecular weight is well-exploited when controlling the mechanical properties of plastics⁹ and the flow properties of polymeric fluids. Block copolymers self-assemble into ordered microphase structures with feature size that is controlled by molecular weight. Such self-assembled morphologies are exploited for nanoscale lithography for electronic and optical devices and for nanoparticle synthesis. All living things are composed of polymeric materials with exquisite molecular organization and functional capabilities that are dictated by the linkage of chemically diverse amino acids into chains. There exist many approaches to controlling molecular organization within such polymeric materials for desirable properties.

It is not surprising that some features of charge transport in conjugated polymers are unique to this family of materials. The mobility in general increases nonlinearly with the degree of polymerization of the polymer. Furthermore, a number of experimental data sets demonstrate that at low fields the Poole–Frenkel effect disappears or even inverts.^{10–13}

We posit that these phenomena reflect the nature of charge transport along a polymer chain and are therefore an expression of the macromolecular nature of the material. We demonstrate that the key physical process controlling mobility is the capacity for a charge to navigate around traps. We simulate the mobility

Received: August 29, 2016

Published: November 10, 2016

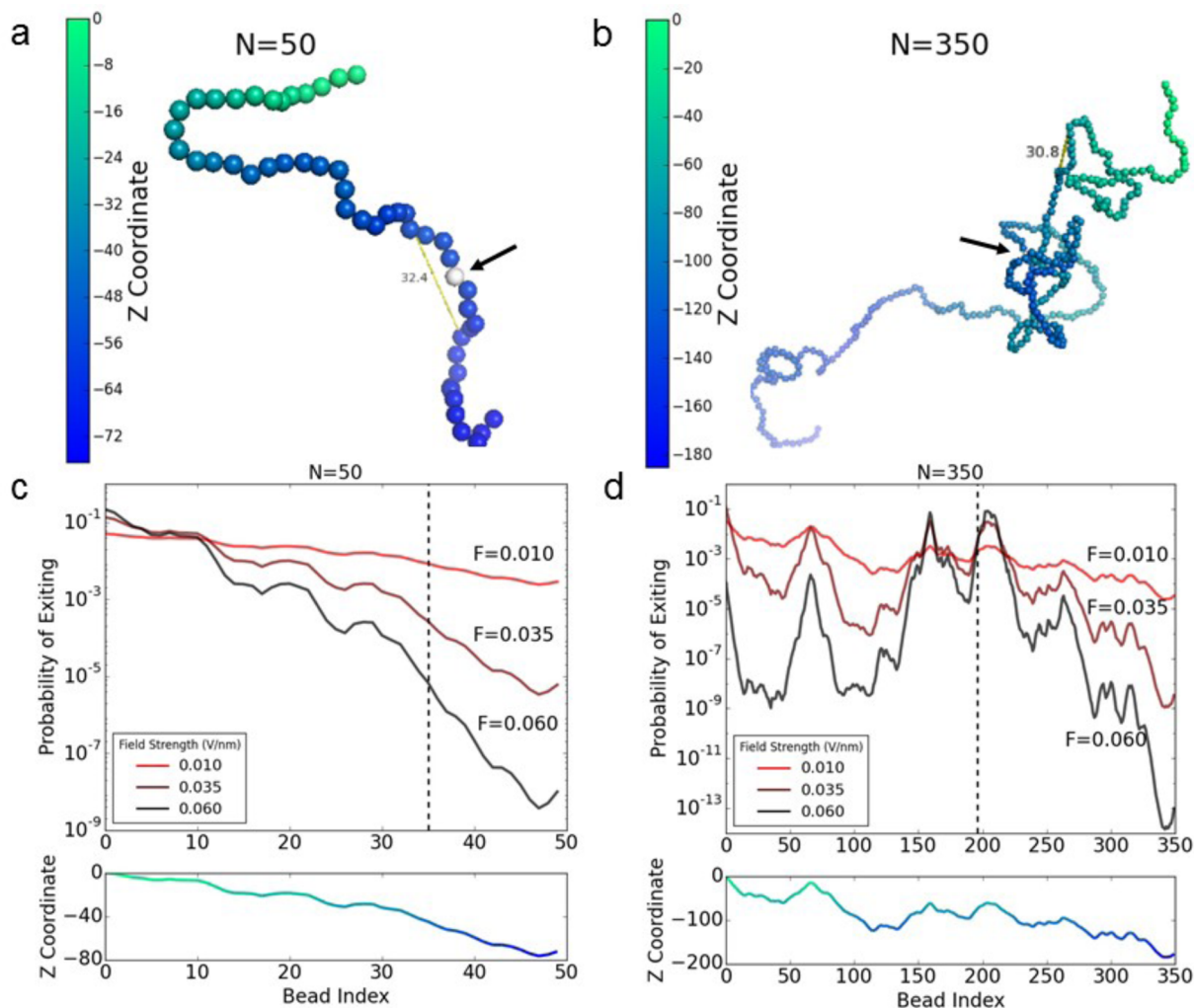


Figure 1. Snapshots of the wormlike chain conformations for the two different molecular weights of 50 beads (a) and 350 beads (b). The color scale represents the z -coordinate (i.e., distance in the field direction). (c, d) Probability of exiting the chain at each bead at low (c) and high (d) molecular weights. The charge was initialized at bead index $i = 35$ for the 50-bead chain and $i = 196$ for the 350-bead chain, as marked by the arrows in panels a and b and dashed lines in panels c and d.

using polymer conformations to describe the intercrystallite amorphous regions and offer explanations of observed trends. Our work shows how the interplay between polymer conformations and charge transport gives rise to unique behaviors. Polymer science has established a wealth of approaches to controlling conformational properties in polymeric materials using thermodynamic and processing techniques. Thus, insights from our model can be exploited for the design and processing of new materials with improved transport by providing a direct connection between the polymer conformational properties and the device-scale performance.

The π -conjugation within conjugated polymers results in chains with considerable structural rigidity. Thus, the conformational properties of conjugated polymers can be modeled using the wormlike chain model.^{14,15} The chains are discretized into beads that represent monomers with length l_0 , and the bending rigidity is dictated by the persistence length l_p . The bending angles are determined from the wormlike chain model probability distribution.¹⁶ The resulting conformation is defined by the bead positions \vec{r}_i , where i runs from 1 to the number of beads N .

We assume that a charge is localized on a single bead and is capable of hopping to either of the neighboring beads or off to a neighboring chain.¹⁶ The hopping rates are determined by Marcus theory.¹⁷ A charge q within a field of magnitude F in the z -direction experiences an energy difference $\Delta G_{i,j}$ between sites i and j , given by

$$\Delta G_{i,j} = -Fq(z_i - z_j) \quad (1)$$

where $z_i = \vec{r}_i \cdot \hat{z}$. The hopping rate from site i to site $i + 1$ along a single chain is

$$k_{i,i\pm 1} = k_i^\pm = \frac{2\pi}{\hbar} \frac{J_0^2}{\sqrt{4\pi\lambda_0 k_B T}} \exp\left[-\frac{(\lambda_0 + \Delta G_{i,i\pm 1})^2}{4k_B T \lambda_0}\right] \quad (2)$$

where J_0 is the electronic coupling between beads, λ_0 is the reorganization energy, and \hbar is the reduced Planck's constant. Each site can also couple to a site on a different chain, with a rate k_{hop} determined by the interchain electronic coupling J_{hop} and reorganization energy λ_{hop} . We assume a constant energy difference $\Delta G_{\text{hop}} = Fq\gamma l_0$ for interchain transfer, where γ is the ratio between the interchain hop distance and the segment length l_0 .

Our dynamic Monte Carlo algorithm for amorphous charge transport bridges the single-chain behavior to charge transport within an amorphous region within a semicrystalline material (see [Supporting Information](#) for details). The charge takes a series of steps along a chain and between chains with the respective hopping rates. If the charge hops off the chain in the amorphous region, a new chain is generated. This procedure continues until the charge reaches a crystal. The goal in our model is to capture chain conformations as the pathways for charge transport, and other contributions, such as energetic disorder and conjugation-length heterogeneity, can be introduced later as refinements.

Our amorphous model acts as input to a semicrystalline model that captures a heterogeneous material with crystalline and amorphous domains (see [Supporting Information](#) for details). The crystalline domains have a charge mobility μ_{agg} . The two-dimensional nature of the grid of crystals aims to approximate the two-dimensional transport within the accumulation layer of a transistor. If the charge enters a crystal from the amorphous region of the film, the distance it travels in the crystal is determined by μ_{agg} and the field direction, after which it exits again to the amorphous region at the appropriate position. We leverage both the amorphous and the semicrystalline versions of our model.

We define a morphological trap as the position where the bead-to-bead orientation is perpendicular to the field.¹⁸ It is instructive to visualize morphological traps for chains of varying length ([Figure 1](#)). When the length Nl_0 is comparable to the persistence length l_p , there are few instances where the polymer bends backward with respect to the field. When $Nl_0 \gg l_p$, there are numerous locations that have traps.

We visualize the traps by examining the exit distribution for three different field strengths (upper panels of [Figures 1c](#) and [1d](#)). For the 50-bead chain, the high probability at a high z -position indicates that the charge is swept toward the end and remains there before exiting. The exit distribution is more balanced at lower fields ($F = 0.01$ V/nm) and skewed at large fields ($F = 0.1$ V/nm). For the 350-bead chain, the probability distribution shows peaks and valleys within the chain that correspond to the traps. The high-field distribution peaks at the trap near the initial position, and the charge is unlikely to make its way around the winding turns to traverse further along the chain. At lower fields, the charge can exit the morphological trap and reaches the upper chain end.

It is commonly observed that mobility is strongly dependent on the molecular weight.^{19,20} Thin-film transistor measurements demonstrate that mobility initially increases with length before leveling off. However, there are few theoretical studies aimed at understanding the influence of chain length on mobility, and existing studies neglect the field, which we demonstrate in [Figure 1](#) to impact charge trapping.

Previous work examines conductivity from a scaling perspective.^{21,22} If the carrier has time to completely explore the chain, the conductivity scales with molecular weight, while if it quickly hops between chains the two are independent. Pearson et al.²² analyze the conductivity by finding the distance a charge diffuses along a chain in the absence of field. Similarly, Carbone et al. analyze several conformation models. In the absence of field, the distance a charge diffuses along a chain depends only on the chain length and the interchain hopping time.²³ None of these studies quantify the effect of field on mobility, limiting their applicability to address experimental field dependence. Furthermore, conformation-dependent trap-

ping shown in [Figure 1](#) is strongly influenced by field and cannot be addressed in the absence of field.

P3HT is an ideal model system to test the theory due to the wealth of experimental data in the literature. In [Figure 2](#), we

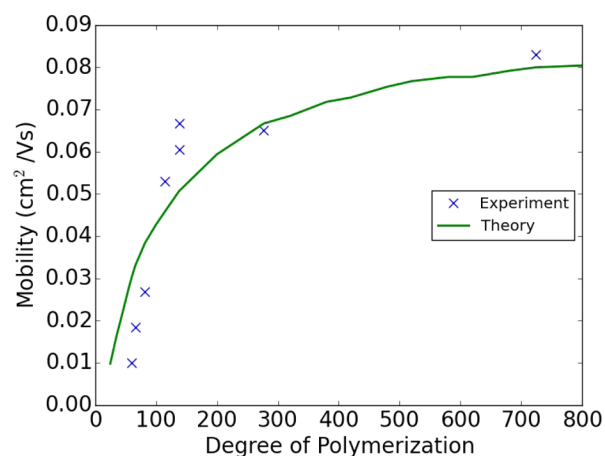


Figure 2. Experimental data and simulated mobility versus chain length. The increase in the mobility is associated with the reduction in the number of chain-end traps between crystallites with increasing chain length.

model mobility data from Chang et al.¹⁹ for P3HT of varying molecular weight. This molecular weight series is synthesized to have consistent regioregularity, and the transistors are fabricated uniformly and characterized by the same group. Under similar conditions as in ref 19 and over a range of comparable molecular weights, the degree of crystallinity of P3HT films is found to be approximately constant.²⁴ Therefore, we fix the degree of crystallinity across all molecular weight values.¹⁹ The fixed parameters used are a fraction crystallinity of 45%, grid size of 15 nm, channel length of 1 μm , $l_0 = 0.4$ nm, $F = 0.025$ V/nm, and $T = 295$ K. The first two parameters are derived from X-ray and absorption measurements,²⁴ while the channel length and field are given parameters of the transistor experiment. The fitted parameters are $l_p = 3.01$ nm, $J_0 = 295$ meV, $\lambda_0 = 368$ meV, $\mu_{\text{agg}} = 0.2895$ cm²/(V s), and $k_{\text{hop}} = 6 \times 10^9$ 1/s.

Another unique feature of polymer semiconductors is the field dependence. In time-of-flight (TOF) measurements, mobility is often measured to have a Poole–Frenkel dependence.²⁵ This type of field dependence is commonly attributed to correlated energetic and positional disorder selected from a Gaussian distribution of site energies.^{10,11} In our conformation-based model, the properties of the wormlike chain also naturally result in this Poole–Frenkel behavior¹⁶ as the chain conformations introduce energetic disorder with position correlations.

However, there are a number of experiments where mobility decreases with increasing field (negative β). Several explanations have been proposed. Diffusive motion becomes significant at low fields and high temperatures, but calculations by Fishchuk et al.²⁶ estimate a critical field ~ 4 orders of magnitude lower than typical fields. Juska et al.²⁷ suggest that several TOF experiments²⁸ may not provide an accurate measurement of long-time mobility and propose using charge extraction by linearly increasing voltage (CELIV).²⁹ Mozer et al.^{10,11} used both CELIV and TOF for P3HT and confirmed a negative field dependence with both techniques. Others

observe similar behavior in P3OT,¹³ PHPS,¹² and doped polymers.^{30,31} Shen et al.³² observe a negative field dependence in P3HT above 120 °C, close to the melting point. Finally, some CELIV reports³³ observe negative field dependence for P3HT over all fields.

We use our amorphous charge-transport model to fit mobility data obtained by Mozer et al.¹¹ at different temperatures and fields (Figure 3). Since the details of the

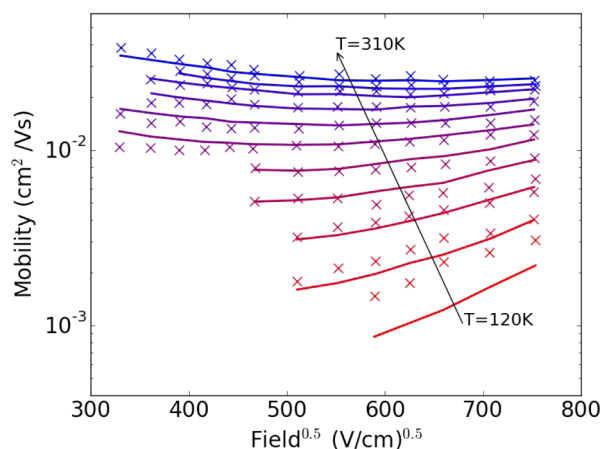


Figure 3. Examples of negative-field-dependent fits to P3HT bulk mobility data using the three-dimensional model. TOF data from Mozer et al.¹¹ and corresponding 3D simulation fit. A molecular weight of $n = 200$ was used.

field dependence are due to the fundamental properties of the amorphous conjugated polymers rather than those of the crystals (see below), we use an entirely amorphous polymer model. The parameters resulting in the best fit were $l_0 = 0.404$ nm, $l_p = 3.19$ nm, $J = 194$ meV, $\lambda_0 = 170$ meV, $J_{\text{hop}} = 2.4$ meV, $\lambda_{\text{hop}} = 378$ meV, and $\gamma = 4.85$.

Charge trapping dictates the impact of molecular weight and electric field on charge transport (Figure 1). Depending on whether trapping occurs at a morphological trap or a chain end, increasing field can be either beneficial or harmful. The field strength controls the overall vertical distance the charge travels. For optimum mobility, the charge should explore the entire chain and locate the furthest point in the field direction. As long as there is somewhere “up” to go, increasing the field increases the rate of movement toward the local maximum: $k_{\text{up}} \propto \exp\left[-\frac{1}{4kT}(\lambda - Fq\delta z)\right]$. This field-dependent hopping rate yields a traditional positive Poole–Frenkel coefficient.

The distance traveled per chain varies with chain length. If the charge is at a local trap on a long chain (i.e., a local maximum), the rate to navigate around the trap (without hopping to a neighboring chain) decreases with increasing field: $k_{\text{down}} \propto \exp\left[-\frac{1}{4kT}(\lambda + Fq\delta z)\right]$. Thus, the charge is less likely to escape the trap at higher fields. In contrast, for a short chain, it is more likely that the charge encounters a chain end as a trap. In this case, transport always improves with higher field, since the charge can more efficiently escape to a new chain: $k_{\text{off}} \propto \exp\left[-\frac{1}{4kT}(\lambda_{\text{off}} + Fq\gamma l_0)\right]$. The molecular weight determines the number of morphological traps, which in turn controls the overall transport behavior with field as a function of the three rates.

This concept of morphological trapping is crucial to understanding the molecular weight dependence of mobility observed in transport measurements, where two broad regimes of behavior emerge. In the first regime, mobility increases sharply with increasing chain length at low chain lengths. The second regime is the saturation of mobility at higher molecular weights. At low molecular weight, large but disconnected crystals are formed, creating traps between grains due to chain ends. As molecular weight increases, more chains are able to bridge these increasingly disordered crystals and charges no longer encounter traps in the intergrain region. Noriega et al.³⁴ suggest that the amount of disorder in the crystals, as measured by paracrystallinity, levels off at around the same length at which the chains become entangled and begin to fold back. Thus, a saturation point in connectivity is reached where transport is limited by interchain hopping.

Our model indicates that the increased connectivity between crystallites is due to persistence-length effects and a reduction of chain ends in the amorphous region with increasing length. Our simulation predicts the concentration of these tie molecules with chain length and persistence length. We track possible routes of a charge exiting a crystal (Figure 4a). Figure 4b shows the fraction of chains that exhibit the routes shown in Figure 4a for varying ratios of the persistence length l_p to the intercrystallite spacing d (ranging from $l_p = 0.25d$ in blue to $l_p = 4d$ in red). The number of tie chains saturates with molecular weight (Figure 4b), mirroring how mobility saturates with molecular weight. As the persistence length l_p increases relative to the intercrystallite spacing, tie chains contain fewer kinks, and the tie-chain fraction at large molecular weights increases (Figure 4b). The role of connectivity can be deduced by comparing semicrystalline simulations with purely amorphous simulations. The latter also show an increase of mobility with chain length, as expected due to polymer conformation and chain-length effects, but the increase is not as significant in magnitude as in the semicrystalline microstructure. Indeed, Li et al.³⁵ observed that in the PBnDT-FTAZ polymer blended with PCBM, which gives rise to a nearly amorphous polymer microstructure, hole mobility increases only about a factor of 2 going from 10 kDa to 60 kDa, in contrast with the semicrystalline P3HT data set where mobility increased by a factor of 10 when molecular weight increased by the same factor.

At low molecular weights, the chain-end effects are the dominant contribution to the mobility trend (inset of Figure 4b). The separation into end-chain and midchain traps is not proportional to the bead distribution. The charge is equally likely to leave a short chain from an end or from the rest of the chain, indicating that the ends play a significant role. The overall likelihood that a charge crosses on a tie molecule also depends on the field strength, and the dependence of the fraction of tie molecules on persistence length becomes stronger with field (Figure S1). This trend is due to the morphological trapping described in Figure 1, where a charge has a higher chance of being stuck in the middle of the chain at higher fields. The distance traveled on a single amorphous chain as a function of field strength initially increases and then decreases due to the prevalence of the morphological trapping effect (Figure S4a).

We expect that the field dependence of mobility should also be influenced by the molecular weight. At shorter chain lengths, the mobility has the traditional Poole–Frenkel dependence and a positive value for β (Figure S4b) because there are no

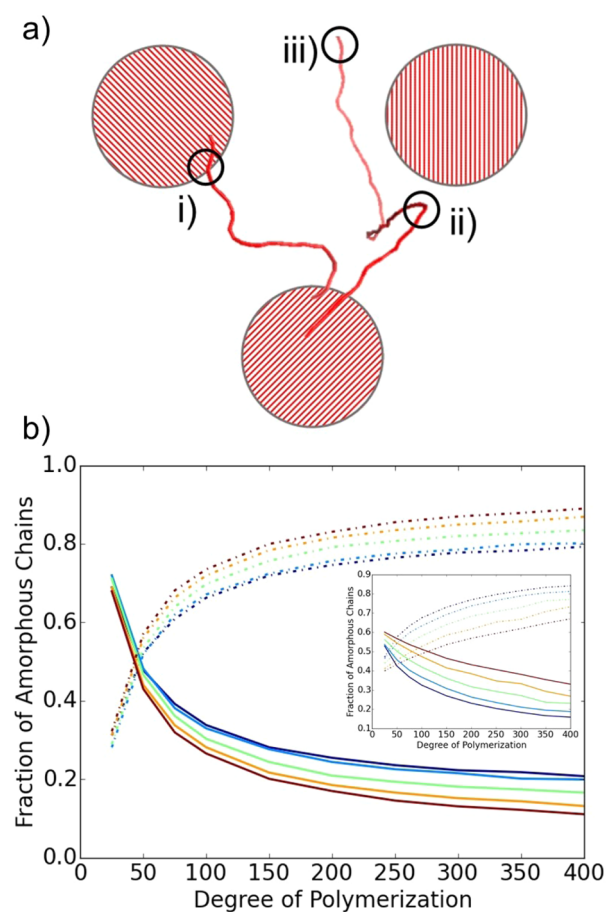


Figure 4. Fraction of charge-chain instances where the charge exited into another crystal or into the amorphous material. (a) Schematic of possible scenarios for single-chain transport resulting in (i) an exit into a crystal, (ii) a jump into the amorphous region from the middle of the chain, or (iii) a jump into the amorphous region from the end of a chain (first and last two beads). In panel b, dashed curves are exiting to a crystal and solid curves exit to amorphous region, while in the inset of panel b dashed curves correspond to midchain hops and solid curves to end-chain hops. The field barrier is slightly higher than the temperature, and the colors indicate a range of intercrystallite spacing from $d = 4l_p$ in blue to $d = 0.25l_p$ in red.

morphological traps to traverse. For the longer chains, the mobility is much less field-dependent overall, and the mobility increases for decreasing field strength at lower field values. Experimentally, several groups observe that lower molecular weight chains have a stronger field dependence, in both field-effect transport measurements (2D transport) and space-charge-limited current measurements (3D transport).^{19,36}

Prior works suggest that the field dependence can be explained within the Gaussian framework by introducing positional disorder into the site energies. Fishchuk et al.^{26,37} explain the negative field dependence within the Gaussian framework by hypothesizing that increased positional disorder creates field-induced “dead ends” in an analogy with directed percolation theories.^{38,39} The increasing field may eliminate the faster percolation routes, in which portions of the critical path require current to run backward against the field. However, the positional disorder introduced in these works^{26,37} is not associated with molecular or microstructural features of the material. The merit of interpreting transport through the lens of our framework is that dead ends are naturally based in the

morphology of the chains as either midchain traps or chain ends. Thus, the model identifies the faster transport path as the route along one connected chain. By demonstrating the molecular origins of traps, it becomes possible to systematically design films that avoid high concentrations of these dead ends. Controlling the mesostructure of semiconducting polymers has offered major performance improvements, and our model physically rationalizes such improvements and suggests a theoretical route for further optimization.

We are currently exploring the impact of on-site energetic disorder in our model. Energetic disorder along the chain leads to a model that varies from our current description (at low variance in the energy) to an effective Gaussian disorder model (at high variance in the energy). The basic trend is that both models capture the Poole–Frenkel effect over a range of fields. However, the inverse Poole–Frenkel is not observed when the spread (or variance) in the site energies is sufficiently large. We will fully explore these effects in our future work.

In conclusion, the dramatic increase of mobility with chain length and the unique features of the field dependence of the mobility reveal that charge transport in polymers is strongly influenced by the chain conformations. The prevalence of traps changes with the length, and the degree to which the charge is able to navigate around these traps depends on the field strength. The direct incorporation of the polymer chain into a transport model ties together molecular and mesoscale properties in explaining complex experimental trends. Well-established approaches to controlling the conformational properties and the mesoscale structure of polymers are instrumental in the fabrication of polymeric materials with desirable mechanical, transport, thermal, and optical properties. This work lays the foundation for leveraging such processing techniques for the predictive design of microstructures that would lead to enhanced electronic properties.

■ ASSOCIATED CONTENT

📄 Supporting Information

The Supporting Information is available free of charge on the ACS Publications website at DOI: [10.1021/acscentsci.6b00251](https://doi.org/10.1021/acscentsci.6b00251).

Details of the algorithmic implementation of model into simulations, procedure for fitting experimental data, and justification of experimentally derived parameters (PDF)

■ AUTHOR INFORMATION

Corresponding Author

*E-mail: ajspakow@stanford.edu.

Notes

The authors declare no competing financial interest.

■ ACKNOWLEDGMENTS

S.A.M. is supported by a Benchmark Stanford Graduate Fellowship. A.S. acknowledges financial support from NSF Award DMR 1205752.

■ REFERENCES

- (1) Yang, Y. M.; Chen, W.; Dou, L.; Chang, W.-H.; Duan, H.-S.; Bob, B.; Li, G.; Yang, Y. High-performance multiple-donor bulk heterojunction solar cells. *Nat. Photonics* **2015**, *9*, 190–198.
- (2) He, Z.; Xiao, B.; Liu, F.; Wu, H.; Yang, Y.; Xiao, S.; Wang, C.; Russell, T. P.; Cao, Y. Single-junction polymer solar cells with high efficiency and photovoltage. *Nat. Photonics* **2015**, *9*, 174–179.

- (3) Sirringhaus, H.; Sakanoue, T.; Chang, J.-F. In *Physics of Organic Semiconductors*; Brütting, W., Adachi, C., Eds.; Wiley-VCH Verlag GmbH & Co. KGaA: 2012; pp 201–238.
- (4) Venkateshvaran, D.; et al. Approaching disorder-free transport in high-mobility conjugated polymers. *Nature* **2014**, *515*, 384–388.
- (5) Kim, G.; Kang, S.-J.; Dutta, G. K.; Han, Y.-K.; Shin, T. J.; Noh, Y.-Y.; Yang, C. A Thienoisindigo-Naphthalene Polymer with Ultrahigh Mobility of 14.4 cm²/Vs That Substantially Exceeds Benchmark Values for Amorphous Silicon Semiconductors. *J. Am. Chem. Soc.* **2014**, *136*, 9477–9483.
- (6) Xie, W.; McGarry, K. A.; Liu, F.; Wu, Y.; Ruden, P. P.; Douglas, C. J.; Frisbie, C. D. High-Mobility Transistors Based on Single Crystals of Isotopically Substituted Rubrene-d₂₈. *J. Phys. Chem. C* **2013**, *117*, 11522–11529.
- (7) Walley, P. A. Electrical conduction in amorphous silicon and germanium. *Thin Solid Films* **1968**, *2*, 327–336.
- (8) Hill, R. M. Poole-Frenkel conduction in amorphous solids. *Philos. Mag.* **1971**, *23*, 59–86.
- (9) Koch, F. P. V.; et al. The impact of molecular weight on microstructure and charge transport in semicrystalline polymer semiconductors-poly(3-hexylthiophene), a model study. *Prog. Polym. Sci.* **2013**, *38*, 1978–1989.
- (10) Mozer, A. J.; Sariciftci, N. S.; Pivrikas, A.; Osterbacka, R.; Juska, G.; Brassat, L.; Bassler, H. Charge carrier mobility in regioregular poly(3-hexylthiophene) probed by transient conductivity techniques: A comparative study. *Phys. Rev. B: Condens. Matter Mater. Phys.* **2005**, *71*, 035214.
- (11) Mozer, A. J.; Sariciftci, N. S. Negative electric field dependence of charge carrier drift mobility in conjugated, semiconducting polymers. *Chem. Phys. Lett.* **2004**, *389*, 438–442.
- (12) Kunimi, Y.; Seki, S.; Tagawa, S. Investigation on hole drift mobility in poly(n-hexylphenylsilane). *Solid State Commun.* **2000**, *114*, 469–472.
- (13) Kazukauskas, V.; Pranaitis, M.; Cyras, V.; Sicot, L.; Kajzar, F. Negative mobility dependence on electric field in poly(3-alkylthiophenes) evidenced by the charge extraction by linearly increasing voltage method. *Thin Solid Films* **2008**, *516*, 8988–8992.
- (14) Kratky, O.; Porod, G. Röntgenuntersuchung Geloster Fadenmoleküle. *Recl. Trav. Chim. Pay. B* **1949**, *68*, 1106–1122.
- (15) Saito, N.; Takahashi, K.; Yunoki, Y. The Statistical Mechanical Theory of Stiff Chains. *J. Phys. Soc. Jpn.* **1967**, *22*, 219–226.
- (16) Noriega, R.; Salleo, A.; Spakowitz, A. J. Chain conformations dictate multiscale charge transport phenomena in disordered semiconducting polymers. *Proc. Natl. Acad. Sci. U. S. A.* **2013**, *110*, 16315–16320.
- (17) Marcus, R. A. On the theory of oxidation-reduction reactions involving electron transfer. I. *J. Chem. Phys.* **1956**, *24*, 966–978.
- (18) Mollinger, S. A.; Krajina, B. A.; Noriega, R.; Salleo, A.; Spakowitz, A. J. Percolation, Tie-Molecules, and the Microstructural Determinants of Charge Transport in Semicrystalline Conjugated Polymers. *ACS Macro Lett.* **2015**, *4*, 708–712.
- (19) Chang, J.-F.; Clark, J.; Zhao, N.; Sirringhaus, H.; Breiby, D. W.; Andreasen, J. W.; Nielsen, M. M.; Giles, M.; Heeney, M.; McCulloch, I. Molecular-weight dependence of interchain polaron delocalization and exciton bandwidth in high-mobility conjugated polymers. *Phys. Rev. B: Condens. Matter Mater. Phys.* **2006**, *74*, 115318.
- (20) Zen, A.; Pflaum, J.; Hirschmann, S.; Zhuang, W.; Jaiser, F.; Asawapirom, U.; Rabe, J. P.; Scherf, U.; Neher, D. Effect of Molecular Weight and Annealing of Poly(3-hexylthiophene)s on the Performance of Organic Field-Effect Transistors. *Adv. Funct. Mater.* **2004**, *14*, 757–764.
- (21) Baughman, R. H.; Shacklette, L. W. Conductivity as a function of conjugation length: Theory and experiment for conducting polymer complexes. *Phys. Rev. B: Condens. Matter Mater. Phys.* **1989**, *39*, 5872–5886.
- (22) Pearson, D. S.; Pincus, P. A.; Heffner, G. W.; Dahman, S. J. Effect of molecular weight and orientation on the conductivity of conjugated polymers. *Macromolecules* **1993**, *26*, 1570–1575.
- (23) Carbone, P.; Troisi, A. Charge Diffusion in Semiconducting Polymers: Analytical Relation between Polymer Rigidity and Time Scales for Intrachain and Interchain Hopping. *J. Phys. Chem. Lett.* **2014**, *5*, 2637–2641.
- (24) Himmelberger, S.; Vandewal, K.; Fei, Z.; Heeney, M.; Salleo, A. Role of Molecular Weight Distribution on Charge Transport in Semiconducting Polymers. *Macromolecules* **2014**, *47*, 7151–7157.
- (25) Rakhmanova, S. V.; Conwell, E. M. Electric-field dependence of mobility in conjugated polymer films. *Appl. Phys. Lett.* **2000**, *76*, 3822–3824.
- (26) Fishchuk, I. I.; Kadashchuk, A.; Bassler, H.; Abkowitz, M. Low-field charge-carrier hopping transport in energetically and positionally disordered organic materials. *Phys. Rev. B: Condens. Matter Mater. Phys.* **2004**, *70*, 245212.
- (27) Juska, G.; Genevicius, K.; Arlauskas, K.; Osterbacka, R.; Stubb, H. Charge transport at low electric fields in π -conjugated polymers. *Phys. Rev. B: Condens. Matter Mater. Phys.* **2002**, *65*, 233208.
- (28) Kaneto, K.; Hatae, K.; Nagamatsu, S.; Takashima, W.; Pandey, S. S.; Endo, K.; Rikukawa, M. Photocarrier Mobility in Regioregular Poly(3-hexylthiophene) Studied by the Time of Flight Method. *Jpn. J. Appl. Phys.* **1999**, *38*, L1188–L1190.
- (29) Juska, G.; Arlauskas, K.; Viliunas, M.; Kocka, J. Extraction Current Transients: New Method of Study of Charge Transport in Microcrystalline Silicon. *Phys. Rev. Lett.* **2000**, *84*, 4946–4949.
- (30) Borsenberger, P. M. Hole transport in mixtures of cyclohexane and bisphenol A polycarbonate. *J. Appl. Phys.* **1990**, *68*, 5682–5686.
- (31) Raj Mohan, S.; Joshi, M. P. Field dependence of hole mobility in TPD-doped polystyrene. *Solid State Commun.* **2006**, *139*, 181–185.
- (32) Shen, X.; Duzhko, V. V.; Russell, T. P. A Study on the Correlation between Structure and Hole Transport in Semi-Crystalline Regioregular P3HT. *Adv. Energy Mater.* **2013**, *3*, 263–270.
- (33) Huang, B.; Glynos, E.; Frieberg, B.; Yang, H.; Green, P. F. Effect of Thickness-Dependent Microstructure on the Out-of-Plane Hole Mobility in Poly(3-Hexylthiophene) Films. *ACS Appl. Mater. Interfaces* **2012**, *4*, 5204–5210.
- (34) Noriega, R.; Rivnay, J.; Vandewal, K.; Koch, F. P. V.; Stingelin, N.; Smith, P.; Toney, M. F.; Salleo, A. A general relationship between disorder, aggregation and charge transport in conjugated polymers. *Nat. Mater.* **2013**, *12*, 1038–1044.
- (35) Li, W.; Yang, L.; Tumbleston, J. R.; Yan, L.; Ade, H.; You, W. Controlling Molecular Weight of a High Efficiency Donor-Acceptor Conjugated Polymer and Understanding Its Significant Impact on Photovoltaic Properties. *Adv. Mater.* **2014**, *26*, 4456–4462.
- (36) Goh, C.; Kline, R. J.; McGehee, M. D.; Kadnikova, E. N.; Fréchet, J. M. J. Molecular-weight-dependent mobilities in regioregular poly(3-hexyl-thiophene) diodes. *Appl. Phys. Lett.* **2005**, *86*, 122110.
- (37) Fishchuk, I. I.; Kadashchuk, A.; Bassler, H. Theory of low-field hopping mobility in organic solids with energetic and positional disorder. *Phys. Status Solidi C* **2006**, *3*, 271–274.
- (38) Bottger, H.; Bryksin, V. V. Investigation of non-Ohmic hopping conduction by methods of percolation theory. *Philos. Mag. B* **1980**, *42*, 297–310.
- (39) Van Lien, N.; Shklovskii, B. I. Hopping conduction in strong electric fields and directed percolation. *Solid State Commun.* **1981**, *38*, 99–102.